

Uncertainties in atmospheric chemistry modelling due to convection parameterisations and subsequent scavenging

H. Tost^{1,2}, M. G. Lawrence¹, C. Brühl¹, P. Jöckel^{1,*}, The GABRIEL Team³, and The SCOUT-O3-DARWIN/ACTIVE Team⁴

¹Atmospheric Chemistry Department, Max Planck Institute for Chemistry, P.O. Box 3060, 55020 Mainz, Germany

²EEWRC, The Cyprus Institute, Nicosia, Cyprus

³Consortium of MPI for Chemistry, Enviscope, MDS, KNMI, STINASU

⁴Consortium of over 75 atmospheric research institutes worldwide

* now at: Deutsches Zentrum für Luft-und Raumfahrt (DLR), Institut für Physik der Atmosphäre, Oberpfaffenhofen, 82234 Weßling, Germany

Received: 13 February 2009 – Published in Atmos. Chem. Phys. Discuss.: 5 May 2009

Revised: 31 January 2010 – Accepted: 8 February 2010 – Published: 19 February 2010

Abstract. Moist convection in global modelling contributes significantly to the transport of energy, momentum, water and trace gases and aerosols within the troposphere. Since convective clouds are on a scale too small to be resolved in a global model their effects have to be parameterised. However, the whole process of moist convection and especially its parameterisations are associated with uncertainties. In contrast to previous studies on the impact of convection on trace gases, which had commonly neglected the convective transport for some or all compounds, we investigate this issue by examining simulations with five different convection schemes. This permits an uncertainty analysis due to the process formulation, without the inconsistencies inherent in entirely neglecting deep convection or convective tracer transport for one or more tracers.

Both the simulated mass fluxes and tracer distributions are analysed. Investigating the distributions of compounds with different characteristics, e.g., lifetime, chemical reactivity, solubility and source distributions, some differences can be attributed directly to the transport of these compounds, whereas others are more related to indirect effects, such as the transport of precursors, chemical reactivity in certain regions, and sink processes.

The model simulation data are compared with the average regional profiles of several measurement campaigns, and in

detail with two campaigns in fall and winter 2005 in Suriname and Australia, respectively.

The shorter-lived a compound is, the larger the differences and consequently the uncertainty due to the convection parameterisation are, as long as it is not completely controlled by local production that is independent of convection and its impacts (e.g. water vapour changes). Whereas for long-lived compounds like CO or O₃ the mean differences between the simulations are less than 25%), differences for short-lived compounds reach up to $\pm 100\%$ with different convection schemes.

A rating of an overall “best” performing scheme is difficult, since the optimal performance depends on the region and compound.

1 Introduction

Moist convection plays an important role in the transport of energy and moisture in the lower atmosphere, where it is a substantial part of global circulation patterns, e.g. the Hadley and the Walker Cells. Furthermore, it contributes crucially to the vertical mixing of the troposphere, especially with respect to atmospheric trace species. Whereas the transport time from the Earth surface into the upper troposphere or vice versa is several days to weeks in the large scale motion flows, the high vertical velocities in up- and downdrafts within deep convective cells can substantially shorten this time to a few hours. In global modelling of the circulation and chemical composition of the atmosphere, these convective clouds can



Correspondence to: H. Tost
(holger.tost@mpic.de)

currently not be explicitly resolved with the state-of-the-art models, rather moist convection is parameterised, which leads to uncertainties in the description of the processes associated with cumulus convection (Arakawa, 2004). The main goal of most of these parameterisations is to “adjust the energy and water budget of a model column to achieve a more stable state of the atmosphere”. A variety of parameterisations for moist convection in the atmosphere exists, some based on similar concepts, and some following rather different approaches (e.g. Arakawa and Schubert, 1974; Kuo, 1974; Tiedtke, 1989; Hack, 1994; Zhang and McFarlane, 1995; Emanuel and Zivkovic-Rothman, 1999; Donner et al., 2001; Bechtold et al., 2001; Lin and Neelin, 2002; Nuber and Graf, 2005). However, a “best” parameterisation cannot be identified easily in general circulation models (GCMs), since the main goal noted above is fulfilled by most of the schemes, at least from a climatological point of view. Even though moist convection is also an important aspect of numerical weather prediction, the requirements for this application are different from those in global modelling of atmospheric chemistry and climate, i.e., the focus is more on the exact location and timing of a convective event.

For atmospheric chemistry the convection scheme is of additional importance, since not only energy and water are redistributed by convection, but also chemical constituents (greenhouse gases, pollutants, aerosols, etc.). The uncertainty associated in the parameterisation formulation of convection has been investigated by Tost et al. (2006b), but restricted to temperature, moisture, and precipitation and in a follow up study (Tost et al., 2007b) focusing on lightning and associated NO_x emissions. Several studies have attempted to address the influence of convection on the chemical composition of the atmosphere by excluding the convective transport of all or specific trace gases.

The pioneering work of a convection scheme intercomparison has been performed by Mahowald et al. (1995), comparing seven convection schemes in detail in a single column model. Artificial tracers with varying characteristic lifetimes have been used, but no interactive chemistry. Furthermore, in that study the convection schemes have only been driven by the prescribed meteorology, but did not have any feedback. Nevertheless, some of the main findings of Mahowald et al. (1995) are fundamental and the present study will not generally contradict those previous results. One of the first studies of addressing the impact of convection with interactive chemistry has been performed by Lelieveld and Crutzen (1994), who found that the O_3 lifetime is strongly influenced by convection. In a follow up study, Lawrence et al. (2003) found a larger effect due to the transport of ozone precursors, especially NO_x , than to the transport of O_3 itself. Other precursors, e.g., isoprene and its degradation products, have been found to be of similar importance by Doherty et al. (2005). For short lived tracers, prototyped by the chemically inactive compound ^{222}Rn , Mahowald et al. (1997) found that the neglect of convective transport leads

to a substantial reduction of its mixing ratio, by $\approx 50\%$ in the upper troposphere. However, as shown by Lawrence and Salzmann (2008), the approach of comparing simulations with and without convective tracer transport only capture part of the effect of deep convective transport, and will therefore fail to give a proper quantification of the effects that are caused by convection in general. An alternate approach is to examine the uncertainty in the process of convective transport and its effects on chemistry by employing a variety of cumulus parameterisations. Thus far, only Zhang et al. (2008) have employed this approach, focusing on the influence of the convection parameterisations on radon, finding differences of the order of 50% between several simulations. This is of the same order as the differences found by Mahowald et al. (1997), in which convective transport was turned off entirely. In this study, we take this research a significant step further, by examining the effects of convective transport on atmospheric chemistry, using a variety of convection schemes, and including the calculation of atmospheric chemistry in both, gas and aqueous phase.

2 Model description and simulation setup

2.1 Model description

In the present study the ECHAM5/MESSy atmospheric chemistry model (EMAC, Jöckel et al., 2006) is applied to investigate the influence of convection parameterisations on atmospheric trace species. EMAC consists of an atmospheric climate model, which is the 5th generation European Centre Hamburg general circulation model (ECHAM5, Roeckner et al., 2006) and the Modular Earth Submodel System (MESSy, Jöckel et al., 2005) to simulate tropospheric and middle atmosphere processes and their interaction with oceans, land and human influences. For this study the standard convection parameterisation of Tiedtke (1989) with the modifications of Nordeng (1994) has been augmented by an interface allowing several other convection schemes to be implemented in parallel (Tost et al., 2006b). To calculate the meteorology and the chemical composition of the atmosphere the MESSy submodels listed in Table 1 have been applied.

Five simulations with a similar configuration have been performed, differing only by the choice of the selected convection parameterisation. This study is based on previous work, in which the influence of the convection parameterisation on the large scale circulation and the hydrological cycle has been investigated (Tost et al., 2006b; Tost, 2006); a rating of the schemes in the EMAC model setup can be derived from this work. The uncertainty in the lightning distribution based on the convection parameterisations has been discussed in Tost et al. (2007b). Following the results therein, the lightning scheme that offers most robustness, i.e., a cloud top height dependent parameterisation (Price et al., 1997) is

Table 1. Applied processes and respective submodels of EMAC.

Process	Submodel name	Reference
Air sea exchange of trace species	AIRSEA	Pozzer et al. (2006)
Large-scale condensation	CLOUD	see Lohmann and Roeckner (1996) Roeckner et al. (2003)
Convection	CONVECT	Tost et al. (2006b)
Convective tracer transport	CVTRANS	see text
²²² Rn cycle	DRADON	P. Jöckel (unpublished)
Dry deposition	DRYDEP	Kerkweg et al. (2006a)
stratospheric H ₂ O and feedback	H2O	see Jöckel et al. (2006)
Photolysis rate calculations	JVAL	see Jöckel et al. (2006)
Lightning NO _x emissions	LNOX	Tost et al. (2007b)
Aerosol microphysics	M7	see Vignati et al. (2004) Kerkweg et al. (2008)
Gas phase chemistry	MECCA	Sander et al. (2005)
Emissions and other boundary conditions	OFFLEM, ONLEM, TNUDGE NCREGRID	Kerkweg et al. (2006b) Jöckel (2006)
Prognostic tracers	TRACER, PTRAC	Jöckel et al. (2008)
QBO nudging	QBO	Jöckel et al. (2006)
Radiation	RAD4ALL	see Jöckel et al. (2006)
Scavenging and cloud/precipitation chemistry	SCAV	Tost et al. (2006a) Tost et al. (2007a)
Aerosol sedimentation	SEDI	Kerkweg et al. (2006a)
Tropopause diagnostics	TROPOP	Jöckel et al. (2006)
Diagnostic tools for the output	various submodels	Jöckel et al., 2010, in preparation

applied in this study. The associated NO_x emission is scaled to produce ≈4 Tg(N)/yr globally from flashes.

To compare the tracer transport using the different convection schemes a ConVective tracer TRANSPort (CVTRANS) algorithm based on Lawrence and Rasch (2005) following the bulk approach (“leaky pipe”) has been implemented. It is equipped with an interface to collect the required updraft and downdraft air mass fluxes and the respective entrainment and detrainment rates of the convection parameterisations. If required it applies an adjustment of these fluxes to guarantee positive definiteness, monotonicity and mass conservation such that the basic equation for updrafts (subscripted “u”) and downdrafts (subscripted “d”) is fulfilled¹:

$$\begin{aligned} F_u^k &= F_u^{k+1} + E_u^k + D_u^k \\ F_d^{k+1} &= F_d^k + E_d^k + D_d^k. \end{aligned} \quad (1)$$

In this equation F_u^k and F_d^k denote the updraft and downdraft mass fluxes at level k respectively, and F_u^{k+1} and F_d^{k-1} the mass fluxes from the layer below and above. E_u^k and E_d^k are the entrainment and D_u^k and D_d^k the detrainment rates from the respective fluxes in this layer. All fluxes are in

¹An additional requirement for the convective tracer transport routine is that the downdrafts may not exceed the updraft, which is usually fulfilled, otherwise an adjustment is applied.

kg/(m²s).² Finally the convective tracer transport in updrafts, downdrafts and the mass balancing subsidence is calculated independently³ from the underlying convection scheme according to the following equation:

$$\begin{aligned} C^k &= ((AM^k - (F_u^k - F_d^k + D_u^k + D_d^k) \times \Delta t) \times C^k \\ &\quad \text{(unaffected by convection)} \\ &\quad + (F_u^k - F_d^k) \times \Delta t \times C^{k-1} \\ &\quad \text{(subsidence)} \\ &\quad + D_u^k \times \Delta t \times C_{ud}^k \\ &\quad \text{(detrained from updraft)} \\ &\quad + D_d^k \times \Delta t \times C_{dd}^k \\ &\quad \text{(detrained from downdraft)} \\ &\quad / AM^k. \end{aligned} \quad (2)$$

The first term determines the fraction of the mixing ratio C^k in a specific layer, which is not directly affected by the convection, the second the effects of the mass balancing subsidence from the layer above (index $k-1$), the third the fraction of detrained species from the updraft with mixing ratio C_{ud}^k ,

²Note that the mass fluxes are defined at the interfaces, e.g., F_u^k is the mass flux at the upper boundary of the grid box, whereas the entrainment and detrainment rates are defined as grid box mean values.

³The mass fluxes and entrainment and detrainment rates are taken from the convection parameterisation.

and the fourth term the fraction of detrained species from the downdraft with mixing ratio C_{dd}^k , with AM^k being the air-mass per unit area in that grid cell. The terms of C_{ud}^k and C_{dd}^k are the mixing ratios within the convective drafts, modified in each layer by entrainment and detrainment (similar to Eq. 1).

The scavenging scheme described by Tost et al. (2006a) has been extended to additionally allow uptake of species onto ice surfaces, the sedimentation of the crystals, i.e., a slow vertical downward transport, the release from the evaporating ice crystals and the transition of species into the liquid phase during melting processes. For the uptake/equilibrium an iterative Langmuir-uptake formulation following the approach of Tabazadeh et al. (1999) has been applied. In this study only HNO_3 is considered for the uptake onto ice particles. The influence of the additional ice uptake of HNO_3 on O_3 is relatively small (of the order of a few %), but for HNO_3 the uptake results in a reduction of up to 30% in the upper troposphere (as shown in the supplement <http://www.atmos-chem-phys.net/10/1931/2010/acp-10-1931-2010-supplement.pdf>), in agreement with previous calculations (v. Kuhlmann and Lawrence, 2006).

2.2 Simulation setup

In this study five simulations have been performed with different convection parameterisations, as listed in Table 2. More details about the schemes and their implementation in the model are described by Tost et al. (2006b). In contrast to the previous studies with this model, the convection schemes have been “tuned” to achieve both, realistic radiation and precipitation fluxes compared to NOAA⁴ and ERBE⁵ (radiation) and CMAP⁶ (precipitation).

A time period of four months is calculated, from 1 September 2005 to 1 January 2006. This period covers two important aircraft campaigns mentioned below in Sect. 3. The meteorology is “nudged” (Newtonian relaxation) towards the temperature, logarithm of the surface pressure, divergence and vorticity of ECMWF analysis data to achieve the same large-scale weather patterns. Direct feedbacks between chemical species and meteorology have been switched off (no variable radiative transfer forcing through O_3 or other trace gases, but using climatological values); therefore the different tracer distributions are solely caused by the convection schemes. However, since water vapour changes with the choice of the convection scheme, meteorology and the chemistry are directly influenced by those changes, e.g., through modified precipitation patterns, radiation feedbacks of water vapour and OH production from H_2O .

⁴National Oceanic and Atmospheric Administration satellite radiation budget data from AVHRR and HIRS instruments

⁵Earth Radiation Budget Experiment

⁶CPC merged analysis project

The model is applied at a resolution of T63 (i.e., with a triangular spherical truncation corresponding to a quadratic Gaussian grid of ≈ 1.875 by 1.875 degrees in latitude and longitude) with 87 vertical hybrid pressure levels up to 0.01 hPa. The application of interactive chemistry in multiple phases and the feedback of the convection on the large-scale circulation extends the study by Mahowald et al. (1995) by allowing many more degrees of freedom in the atmospheric system.

3 Observational data

Two different approaches of comparisons to observational data are performed within this study:

- a comparison to a collection of flight campaign data, compiled by Emmons et al. (2000) (updated by the same authors to include more recent data). These data are more spatially representative, but with the drawback that they originate from several years, i.e. the meteorological conditions are not necessarily reproduced by the simulations. Only data for the appropriate seasons have been included in the analysis comparable to the approach chosen by Jöckel et al. (2006).
- a comparison with flight data of campaigns performed during the simulation period:
 - a comparison with flight data from the GABRIEL campaign (October 2005, Lelieveld et al., 2008) in Suriname and the Guayanas in South America: 10 flights from the lower to the upper troposphere have been conducted, observing H_2O , O_3 , HCHO , CO , HO_x , NO_x , and several organic compounds in combination with ground based measurements; for this analysis only the flight data have been used. Even though the measurements were performed during the dry season (with ≈ 100 mm precipitation per month), local convection was present during almost all of the days. Investigations of convection have not been the main focus of this campaign and convective towers have been avoided for the flight tracks, but during one flight the outflow of convection has been explicitly measured (see Bozem et al., 2010, in preparation).
 - a comparison with flight data from the SCOUT-O3-ACTIVE campaign in Darwin, Australia (December 2005, Vaughan et al., 2008; Brunner et al., 2009). During this joint campaign convection (with emphasis on the Hector system) and large-scale motions, as well as the chemical composition of the atmosphere have been characterised with the help of four aircraft, radio and ozone sondes and ground based measurements; for our analysis flight and sonde data has been used.

Table 2. Convection schemes applied in the individual simulations.

Simulation name	description and references
T1	Tiedtke (1989) with modifications of Nordeng (1994)
EC	IFS cycle 29r1b from the ECMWF (Bechtold et al., 2004)
Ema	Emanuel and Zivkovic-Rothman (1999)
ZHW	a combination of the schemes of Zhang and McFarlane (1995) and Hack (1994) with a modification from Wilcox (2003) for the Zhang and McFarlane (1995) part
B1	Bechtold et al. (2001)

For the latter two campaigns the simulated meteorology is in agreement with the observed one, since the model is “nudged” towards the ECMWF analysis, but the region investigated contains only very few grid boxes and is therefore spatially not very representative.

The combination of the three datasets allow the evaluation of the model simulations with the focus on convective activity.

4 Results

4.1 Global mass fluxes

A major part of the vertical redistribution of trace species in the troposphere is caused by the overturning of air in the convective systems. Consequently, the global convective mass fluxes, which cannot be measured well, are an indicator for the strength of the vertical transport of constituents. Since within one model column the air mass is conserved within one model time step, convection leads only to a redistribution of tracers (due to combined updraft, downdraft and subsidence mass fluxes). The zonal average updraft mass fluxes (time average over the 4 month simulation time, both convective and non-convective events) with the different convection schemes are shown in Fig. 1a. Each bar represents an average over 30° latitude from the individual simulations: e.g. the first bar on the left is the average between 90° S and 60° S for the T1 simulation, the second for the EC simulation, etc. and the sixth bar represents the average between 60° S and 30° S for the T1 simulation. Figures with non-binned zonal averages (and relative differences to the T1 simulation), the full zonal average figures and relative differences to the T1 simulation for all schemes are part of the electronic supplement (<http://www.atmos-chem-phys.net/10/1931/2010/acp-10-1931-2010-supplement.pdf>), which also includes a picture of the average updraft mass flux profiles.

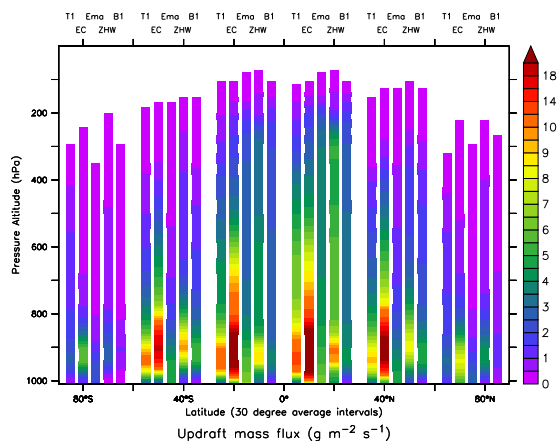
In all simulations the deep convection in the tropics is evident, reaching almost up to the tropopause. The ITCZ in the Atlantic and the Pacific (including the corresponding shift in latitude) causes a two-peak shaped distribution in the trop-

ics. Additionally, there is intense convection in the South Pacific Convergence Zone (SPCZ). Furthermore, in addition to the almost zonally omnipresent shallow convection, enhanced deep convective activity is calculated in the midlatitude storm tracks also up to the tropopause which is at lower altitude.

However, both the absolute strength of the convection in terms of the average mass fluxes and in terms of the frequency distribution (Fig. 1b) and the average convective cloud top height (and consequently the outflow height) depend strongly on the selected convection schemes. For instance, the overall strength in the EC simulation is much larger than in all others (with an even more enhanced shallow convective fraction), especially with much higher occurrences of high mass fluxes at the lower altitudes. In contrast, Ema shows weaker overall convective activity both, in terms of mass flux strength and frequency. B1 shows a lower frequency of the low mass fluxes, which in total lead also to a weaker overturning, however the strong convective events occur as often as in T1 and ZHW. This is further supported by the frequency distributions of the updraft mass fluxes at various altitudes (850 hPa, 500 hPa, 250 hPa, 150 hPa) which are shown in the supplement (<http://www.atmos-chem-phys.net/10/1931/2010/acp-10-1931-2010-supplement.pdf>). The stronger mass fluxes in the upper troposphere found in the ZHW and B1 simulation cause a stronger transport into the upper troposphere. Whereas, however the B1 mass flux originates from the boundary layer (having continuously high mass flux values), representing an almost undiluted transport of boundary layer air into the UTLS (upper troposphere – lower stratosphere region), the ZHW simulation shows sometimes a small increase in the mass flux above 350 hPa, which is mainly caused by the activation of the Hack (1994) part of the scheme (local instabilities which are in the other simulations are stabilised by the large-scale cloud scheme (compare Tost et al., 2006b)). This represents an efficient overturning of air in the middle and upper troposphere, but not necessarily transport of surface air into the UTLS.

This is partly a consequence of the applied “tuning” mentioned above, since the radiation balance can be perturbed with increasing convective activity. This aspect will be discussed in more detail below. ZHW and B1 are characterised

a) Zonal average updraft mass fluxes



b) Frequency distribution of vertically averaged mass fluxes

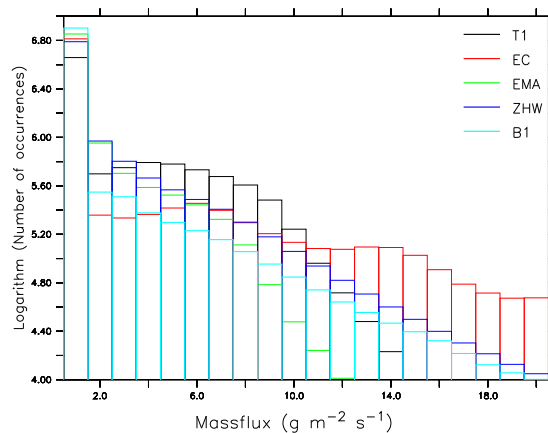


Fig. 1. 4 months average (September–December 2005) of the zonal average updraft mass fluxes (binned into 30° bins) for the five simulations in $\text{g}/(\text{m}^2\text{s})$ (a) and frequency distribution of the 4 months vertically averaged updraft mass fluxes (b).

by the deepest convective activity with substantial mass fluxes up to 200 hPa or even higher. In contrast, T1 convection generally peaks a little lower, especially in the extratropics. Ema, ZHW, and B1 hardly calculate convection in the polar regions, in contrast to T1 and the shallow convective activity of EC.

Even though the mass fluxes are different in all the simulations, in none of them is a significant mass flux over the tropopause computed, i.e., the overshooting events injecting air mass and consequently tracers into the stratosphere are almost negligible, comparable to the findings of Lelieveld et al. (2007).

The corresponding downward mass fluxes (displayed in the supplement <http://www.atmos-chem-phys.net/10/1931/2010/acp-10-1931-2010-supplement.pdf>) also show different spatial distributions, but are of similar strength, within about a factor of two, in all simulations. Especially in the Ema simulation, the downdrafts are weaker in the upper troposphere, causing a slower downward transport of trace species from the UT region. Since the updrafts are balanced by the downdrafts and the mass balancing subsidence (see Eq. 2), the overturning time is longer in the simulations with smaller mass fluxes (both upward and downward). In combination with the chemical lifetime this has implications for the vertical distribution of tracers.

4.2 Tracer distributions

In the real atmosphere the budget of many trace gases is dominated by chemistry. Chemical reactions can mask the differences in transport, but can also amplify those signals. Furthermore, scavenging, liquid phase reactions, and downward transport in hydrometeors (and their potential re-evaporation and subsequent release of species) have an additional impact on the trace species budgets. Since the lat-

ter process depends on liquid and frozen water (clouds and precipitation), which are determined differently in the individual convection schemes, these contribute substantially to the differences in the vertical distributions of many compounds. Therefore, both chemically inactive and reactive tracers as well as moderately and highly soluble tracers will be analysed. This allows an estimate of the relative importance and counter-effects of transport, chemistry and wet removal from the atmosphere. The global distributions as well as comparison with measurement data are provided to estimate the uncertainty originating from the convection parameterisations and rate the convection schemes. Since the analysis, whether the schemes are suitable for simulating a stable atmospheric state has been performed by Tost et al. (2006b), the precipitation and radiation distributions (shown in the supplement <http://www.atmos-chem-phys.net/10/1931/2010/acp-10-1931-2010-supplement.pdf>) will not be discussed in detail.

4.2.1 Global perspective

Figure 2 depicts the differences for the discussed compounds in a summarising way. All data have been averaged in time and longitude. Furthermore, the average for 30° latitude bands have been calculated. These are shown for each simulation in the corresponding latitude ranges. The first bar represents the absolute values for the compound in the T1 simulation (using the colour scale on the left hand side), the other bars in that latitude bin the relative difference in % to the reference values of the T1 simulation $((X-T1)/T1 \cdot 100)$, using the colour scale on the right. Each bar is marked with its corresponding simulation name in the upper row of the graph. The un-binned zonal averages and difference plots are part of the supplement (<http://www.atmos-chem-phys.net/10/1931/2010/acp-10-1931-2010-supplement.pdf>).

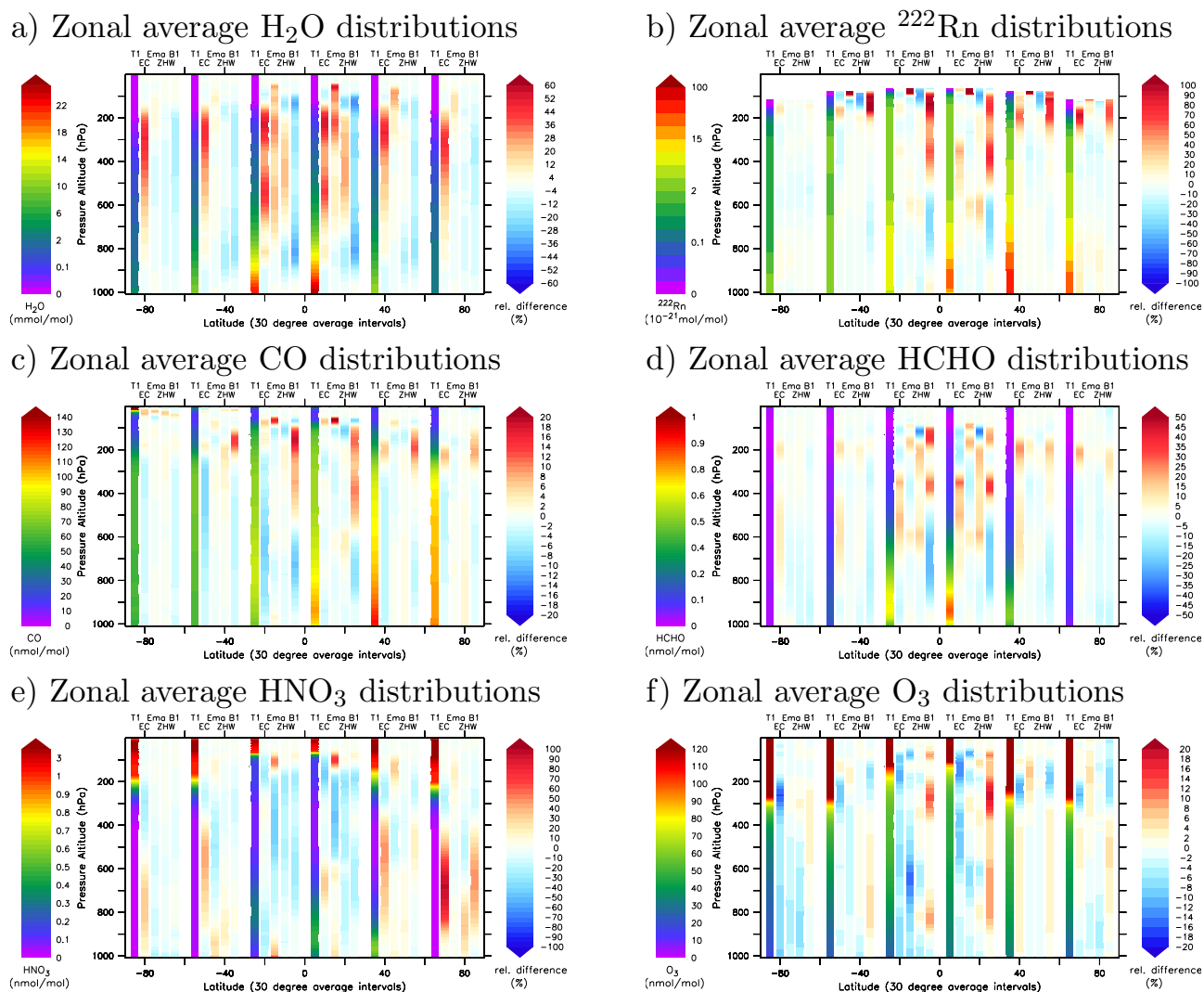


Fig. 2. 4 months average (September–December 2005) of the zonal average concentration of various compounds. The vertical axis depicts pressure altitude, and each bar on the horizontal axis represents an average over 30° latitude (90° S to 60° S, 60° S to 30° S, etc.) for all the simulations as indicated in the top row of the graphs. The first bar in each bin shows the absolute values for the respective compound in the T1 simulation (reference) using the colour bar on the left for the scale. The other four bars in each bin show the relative difference to the reference in %, using the colour scale on the right hand side of the graphs. Panel (a) depicts H₂O, (b) ²²²Rn, (c) CO, (d) HCHO, (e) HNO₃, (f) O₃.

Chemically inactive tracers:

(a) H₂O:

Water vapour is the driving force for moist convective activity, therefore the differences in the moisture distribution caused by the convection schemes are relevant for addressing the uncertainty due to the convection parameterisation in an atmospheric chemistry general circulation model. In the current setup the chemical contribution to H₂O is neglected: the chemical production of H₂O from CH₄ oxidation (relevant mostly for the stratosphere) is prescribed as a climatological tendency. Furthermore, H₂O is not consumed by chemical

reactions. However, the meteorological feedbacks (radiation and the hydrological cycle) from the deep convection parameterisation cannot be eliminated due to their close relationship to the convective dynamics. Since H₂O is a primary source of OH (H₂O+O¹D→2OH), the main oxidant in the lower atmosphere, it also strongly impacts the oxidation capacity and influences almost all chemically reactive compounds. For an evaluation of the water vapour distribution we refer to Jöckel et al. (2006) and Lelieveld et al. (2007), whereas the impact of the convection scheme on simulated water vapour columns were compared with GOME satellite data by Tost et al. (2006b).

All simulations (Fig. 2a) show the typical distribution of water vapour, i.e. highest values in the tropics and a decrease with altitude and polewards. Note that the largest differences occur in the regions with lowest absolute values, being therefore not necessarily relevant for climate⁷. The largest differences caused by the different convection schemes occur in the tropical middle and upper troposphere: from a substantial higher value in the EC simulation to lightly enhanced values in Ema and ZHW and lower values in B1. However, in the EC simulation the larger moisture content is not restricted to the tropics, but is obvious at all latitudes in the middle and upper troposphere, indicating a moister atmosphere, in agreement with the findings by Tost et al. (2006b), where a larger integrated water vapour column was analysed. The moisture is larger up to 40% in EC, i.e. it is substantial, being detrained from the strong shallow convection in this simulation. Ema and ZHW show a smaller moisture enhancement in the tropics than EC, but still larger values compared to the T1 simulation, whereas in the high latitudes a very small lowering of H₂O is obvious. Higher values for both simulations in the upper troposphere are due to the higher outflow level, i.e. the convection is reaching deeper more often, as shown also by the frequency distribution at 250 hPa in the supplement (<http://www.atmos-chem-phys.net/10/1931/2010/acp-10-1931-2010-supplement.pdf>). The diminution of water vapour in the UTLS region in the ZHW simulation results from the activation of the Hack (1994) part of the convection scheme, causing condensation and hence stronger removal of moisture by precipitation. The B1 simulation is characterised by lower moisture values almost everywhere in the troposphere, but most pronounced in the tropics. Weaker updraft mass fluxes result in less transport of moisture to the top of the boundary layer and into the free and upper troposphere. The condensation threshold of this scheme is lower, leading to a similar precipitation production with weaker convective activity and hence a drier atmosphere.

(b) ²²²Rn:

²²²Rn is used as a standard tracer to analyse (continental) convection (Jacob and Prather, 1990) since it is chemically inactive, insoluble, but decays radioactively with a lifetime of ≈3.8 days. These properties make it susceptible to transport alone, i.e. with its help it is possible to deduce the transport characteristics of the convection schemes. Furthermore, some indications for the differences in the convective cloud top and therefore the outflow height can be drawn from the analysis. The emission is set to 1 atom/(cm s) over land and zero over water and ice in this study. However, only very few measurements of vertical profiles of ²²²Rn are available. In a previous study (Tost, 2006) it was found that the simulated vertical profiles differed substantially when alternative con-

vection schemes were applied, but were all within the large scatter of the few available measurement data.

The mixing ratios (depicted in Fig. 2b) are highest in the Northern Hemisphere close to the surface due to the higher land fraction and therefore larger the ²²²Rn emissions⁸. With increasing altitude the Radon content of the atmosphere decreases due to its radioactive decay. In the ITCZ higher mixing ratios can be found in the upper troposphere due to the fast convective transport of air on shorter timescales than the decay rate. Also in the Northern Hemisphere (from 30° to 60° N) a substantial amount of ²²²Rn reaches the upper troposphere due to the nearby emission source and the lifting of air masses due to frontal convective activity and large-scale motion in the conveyor belts.

Some of the large relative differences in the UTLS region result from the small absolute values, hence small changes in the mixing ratio result in large relative differences. The relative changes in the EC simulation to the T1 reference are overall small; near the surface they are slightly positive in the extratropics and negative in the tropics. An enhancement occurs in the tropics in the upper troposphere (between 400 and 300 hPa). This is caused by stronger shallow convection transporting more ²²²Rn-rich air into the middle troposphere, decreasing the overturning time. The differences between Ema and T1 are even smaller: there is only a slight increase in Radon mixing ratios from the equator to 30° N at around 600 hPa. Here the updrafts in the Ema simulation are slightly weaker than in T1, resulting in a less efficient transport into the upper troposphere and a detrainment at this altitude. The ZHW simulation shows a similar behaviour as Ema as explained above. However, again the activation of the Hack (1994) part of the scheme in the tropical uppermost troposphere results in an efficient mixing of ²²²Rn resulting in the slightly higher values in the TTL. The differences of the B1 simulation to T1 in the tropics are much larger. They are caused by an almost undiluted transport of boundary layer air with enhanced ²²²Rn mixing ratios into the upper troposphere. The weak mixing between 800 and 500 hPa (analysed from the entrainment and detrainment rates) inhibits release of Radon in the middle troposphere (causing a lower mixing ratio up to 500 hPa) and leads to the larger values in the upper troposphere from the outflow; this causes a more C-shape like profile than in the other simulations (see supplement <http://www.atmos-chem-phys.net/10/1931/2010/acp-10-1931-2010-supplement.pdf>).

Most of the atmospheric ²²²Rn is located in the troposphere; however the choice of the convection scheme alters the fraction reaching the upper troposphere, whereas the total atmospheric burden is similar in all simulations since it depends only on the amount that enters the stratosphere, which is small due the short decay time. Table 3 depicts the upper tropospheric burden (500 hPa to the tropopause)

⁷They are potentially relevant for climate due to additional cloud formation (e.g., cirrus formation in the upper troposphere).

⁸Note the different scales for both, absolute values and relative differences, compared to H₂O.

and its fraction of the total atmospheric radon burden. The difference in the UT burden exceeds 40% between the B1 (highest value) and the Ema simulation (lowest value). Furthermore, with 22.6% a substantially larger fraction of the total atmospheric ^{222}Rn is located between the 500 hPa and the tropopause level in the B1 simulation. The fraction for the other schemes is quite similar as for T1. This additionally supports our finding that B1 simulates a stronger transport of boundary layer air (enriched in radon) into the upper troposphere. Except for the B1 simulation, the total upper tropospheric burden does not depend substantially on the selected convection parameterisation. The spatial differences, however, are of a similar magnitude as found by Zhang et al. (2008). Overall, even though the distribution of the ^{222}Rn mixing ratios is similar with the different convection schemes (with an exception of the Bechtold scheme), the local absolute values can vary by up to a factor of two.

Chemically reactive tracers:

(a) CO:

CO has a relatively long lifetime and is therefore suitable for addressing questions of convective and long range transport. However, in contrast to ^{222}Rn it is not chemically inactive, but is oxidised mainly by OH. Consequently, the carbon monoxide mixing ratio is also dependent on the OH distribution, which is dominated by local processes and the water vapour concentrations (see above). The mixing ratio in the T1 simulation, shown in Fig. 2c, follows a similar distribution as ^{222}Rn ⁹, since most of the emissions are continental with enhanced fluxes from the industrialised countries of the Northern Hemisphere. Furthermore, biomass burning injects CO in regions of high convective activity in the tropics. The global mean profile of CO (see supplement: <http://www.atmos-chem-phys.net/10/1931/2010/acp-10-1931-2010-supplement.pdf>) is similar in all simulations: a slight increase in the boundary layer and a slow decrease up to almost 300 hPa, followed by a strong decrease up to 40 hPa. Above that, the upper atmospheric source of CO by photodissociation of CO_2 causes a strong increase in the carbon monoxide mixing ratios, especially in high latitude spring.

The generally lower values of CO in the EC simulation compared to T1 are mostly caused by the higher H_2O content and hence an increased OH production leading to an enhanced oxidation of CO to CO_2 . This effect is strongest in the Southern Hemisphere, especially between 30°S and 0° ; on the other side of the equator this effect is less pronounced. This can partly be explained by more pollutants being available in the Northern Hemisphere chemically scavenging the additional OH by faster reactions, such that this

⁹Note, that for CO the scale is linear, and that the relative differences range only between $\pm 20\%$.

Table 3. 4 month average of the upper tropospheric (from the 500 hPa level to the tropopause) ^{222}Rn burden (in g) and its fraction of the total radon burden (in %). The total burden is similar in all simulations ($\approx 209\text{ g}$).

Simulation	Burden	Fraction of total burden above 500 hPa
T1	34.8	16.7
EC	36.8	17.3
Ema	33.4	16.0
ZHW	34.7	16.5
B1	47.1	22.6

effect is buffered. The small differences of CO in Ema and ZHW compared to T1 are not statistically significant and can therefore not directly be attributed to the exchange of the convection parameterisation (and its chemical feedbacks via OH). In contrast to this, the differences in the B1 simulation are much larger and comparable to the findings for ^{222}Rn , i.e. an almost undiluted transport of CO-rich boundary layer air into the TTL without efficient entrainment and detrainment in the middle troposphere. Furthermore, the reduced moisture causes a slightly smaller OH production, and therefore increases the CO lifetime and consequently its upper tropospheric burden.

Due to its long lifetime compared to the convective transport time, the influence of the choice of the convection parameterisation on CO is limited to $\pm 20\%$, but in addition to the vertical transport the effects of changes in OH are of similar importance, as well as horizontal transport.

(b) HCHO:

Formaldehyde (Fig. 2d) is chosen as an exemplary species that is chemically more reactive than CO. HCHO reacts with OH, halogens, NO_3 and photolyses in two different pathways. Therefore all changes in the actinic flux by chemical compounds and water (clouds, water vapour) directly and indirectly influence the HCHO budget. The distribution is dependent on the convective transport of precursors and the compound itself, but additionally it is moderately soluble. Therefore, scavenging and subsequent rainout play a significant role for the global patterns adding another source of uncertainty related to the convection schemes namely cloud and precipitation water. The highest values of HCHO occur in the tropics and subtropics, near the surface due to the enhanced hydrocarbon emissions from both natural (isoprene) and anthropogenic (propane, butane) sources and their subsequent degradation. With increasing altitude the photolysis gains in importance in the destruction of HCHO as well as the lower precursor mixing ratios (hydrocarbons), causing the decrease in the HCHO mixing ratios. The EC simulation shows higher values of HCHO mainly in the middle and upper troposphere due to the enhanced OH

(see supplement <http://www.atmos-chem-phys.net/10/1931/2010/acp-10-1931-2010-supplement.pdf>), which causes a faster degradation of hydrocarbons into formaldehyde. The lower values in the tropical tropopause region correlate well with low OH values in the same region (always compared to the reference T1). However, in the lower troposphere lower values than in T1 are calculated. Since the convective mass fluxes are stronger in this area, the more efficient convective transport leads to an additional enhancement of HCHO in the middle troposphere, and consequently a reduction in the boundary layer. This effect outweighs the chemical effects, since these patterns are different in OH and HCHO. Furthermore, the precipitation in ECMWF is less intense in the tropics, causing a weaker downward transport of HCHO within hydrometeors and their subsequent release due to evaporation and the lower solubility at higher temperatures. The small enhancement in the upper tropical troposphere in Ema compared to T1 results from the higher outflow height, and the lower values below are very well correlated with the higher OH values (see supplement: <http://www.atmos-chem-phys.net/10/1931/2010/acp-10-1931-2010-supplement.pdf>), destroying the available HCHO. In the ZHW simulation HCHO has larger values than T1 in the middle tropical troposphere. Again, this is also correlated with enhanced OH mixing ratios, but in this case the combination of convective transport of HCHO precursors and their subsequent oxidation (forming formaldehyde) counterbalances the HCHO depletion. For the B1 simulation the characteristic features of less diluted transport of boundary layer air yield enhanced upper tropospheric HCHO levels compared to T1. Additionally, the corresponding OH concentrations are lower in that region, leading to a less efficient degradation, such that the convective transport dominates the tropical formaldehyde distribution.

(c) HNO₃:

For the distribution of nitric acid (Fig. 2e) another aspect has to be considered in addition to convective transport of HNO₃ and its precursors, chemistry (mainly reaction with OH and photolysis; however the chemistry of the nitric acid precursors is much more complicated), scavenging and wet deposition: namely the uptake on ice particles. Depending on the detailed treatment of cloud and precipitating ice in the convection parameterisations this yields yet another source of uncertainty related to the convection scheme. In contrast to the tracers analysed before, nitric acid has an increasing concentration in the stratosphere, hence upper tropospheric mixing ratios can be influenced by transport from the stratosphere into the troposphere (only relevant in the midlatitudes due to the circulation patterns).

In the T1 simulation enhanced HNO₃ mixing ratios are found near the surface in the Northern Hemisphere, due to the industrial NO_x emissions, and also elevated in the tropics due to biomass burning and lightning sources of nitric

acid precursors. Upper tropospheric values are relatively low, due to the uptake on ice particles and the subsequent removal on the surface of these particles by precipitation and sedimentation. The global average vertical profiles are similar with all convection schemes, having an S-shape. EC shows a substantial relative increase in the lower and mid troposphere of the extratropics, most pronounced in the arctic. However, since the absolute values of HNO₃ are low, relative changes appear to be very large. In the tropics the situation is different: in the southern part (−30° to 0°) a reduction in nitric acid concentration is simulated from the surface (strongest at low altitude) to the tropopause, mainly because of the enhanced shallow convection and subsequent scavenging by clouds. The change in precipitation compared to T1 on the Northern Hemisphere leads to the enhanced HNO₃ values at around 10° N. In the Ema simulation lower HNO₃ mixing ratios are found in the tropical upper troposphere due to enhanced uptake on ice surfaces, whereas in the boundary layer everywhere a higher HNO₃ content is calculated. In the tropical lower troposphere (below 600 hPa) a substantial increase is calculated, originating from the more intense convection in the biomass burning regions of central Africa, where the emitted NO_x is efficiently transformed into HNO₃ by the enhanced OH levels at the surface and above 700 hPa. ZHW is characterised by mainly lower values in the tropics, since the emissions of nitric acid precursors in the tropics are located over the continents. In these places the convection is more intense, and hence the HNO₃ formed is immediately scavenged by the strong precipitation, whereas the weaker convection over the oceans does not affect the high HNO₃ regions that much. The relative enhancement polewards of 40° is located in regions with lower absolute values and below 600 hPa, such that deep convection cannot be the dominant process. The B1 simulation shows also lower values in the tropics, but enhancements in the polar regions. The tropical patterns are caused by chemistry, i.e. the undiluted transport as seen for other compounds brings surface HNO₃ into the UTLS, where the photolytic destruction is quite efficient, and also the uptake on the ice surfaces, since using this scheme a higher ice water content is calculated (not shown). As before the relative enhancement in the polar regions corresponds to small absolute changes in the HNO₃ content of the atmosphere.

(d) O₃:

Finally, ozone (Fig. 2f) has been selected as a compound in which all of the effects are combined, mainly through the indirect effects on the precursors. The characteristic patterns of the vertical gradient towards the higher values in the stratosphere with a more efficient downward transport in the subtropical subsidence regions are reproduced by the T1 simulation and have been evaluated in detail by Jöckel et al. (2006).

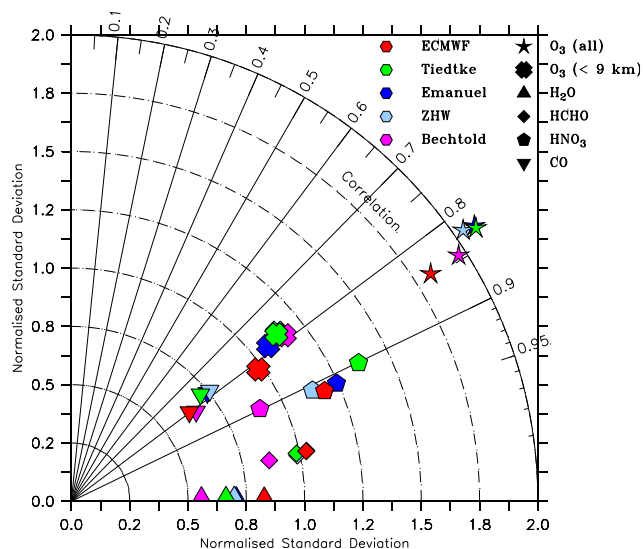
Table 4. 4 month average of the tropospheric O₃ burden (in Tg) from the surface to the tropopause.

Simulation	Burden
T1	331.7
EC	318.8
Ema	324.5
ZHW	328.6
B1	342.1

The differences in the other simulations are not straightforward to explain, due to the multitude of direct and indirect effects. In total they do not exceed a relative change of 25%. This results mainly from the substantially longer chemical lifetime of O₃ compared to the transport times of convection. However, most of the chemical ozone precursors have a shorter lifetime, mainly causing those differences. In the EC simulation there is mostly a reduction of O₃ except in the Northern Hemisphere. The strongest reduction is in the tropics due to the enhanced OH levels and in the tropopause region, where due to the shifts in meteorology the stratosphere – troposphere exchange is altered compared to T1¹⁰. In the Ema simulation the strongest differences occur in the tropics below 600 hPa, likely to be caused by a less efficient transport of O₃ precursors to that altitude. All changes in the ZHW simulation are relatively small. Even though the differences to T1 in the distribution of convection are large, especially the land – sea patterns, the ozone distribution is only slightly affected. However, since O₃ precursors are mostly emitted over the continents, where convection is stronger than in the other parameterisations (and mainly the oceanic convection is underestimated with this scheme), the convection parameterisation nevertheless leads to a realistic efficient mixing of ozone and its precursors in the troposphere. The differences of B1 to T1 are largest. Generally, O₃ is enhanced due to the lower H₂O and OH levels, causing a weaker chemical ozone destruction. This is most pronounced in the tropical upper troposphere. Furthermore, the almost undiluted transport of boundary layer air in convection results in an additional local O₃ production at a faster reaction rate than close to the surface, outweighing the lower ozone content of the air near the surface.

Calculating the tropospheric ozone burden (see Table 4) the total differences are below 8%, with B1 being highest (due to the lowest water vapour content) and EC having the lowest value (due to the high moisture content, destroying tropospheric ozone). These differences are considerably smaller than those of ²²²Rn noted earlier (Table 3). The differences in the tropospheric ozone burden are all smaller than

¹⁰Since the absolute values entering from the stratosphere are large due to the strong gradient, this effect shows up strongly in the relative differences.

**Fig. 3.** Taylor diagram of the comparison between aircraft data from the Emmons et al. (2000) database and the simulations using the different convection parameterisations.

the range found in previous studies in which the convective transport of ozone and/or its precursors has been completely neglected, ranging from –20% to +12% (Lelieveld and Crutzen, 1994; Lawrence et al., 2003; Doherty et al., 2005).

In general, for O₃ the overall picture is too complex to directly associate specific patterns with physical and chemical processes. However, it can be seen that the choice of the convection parameterisation results in a non-negligible uncertainty of 5 to 25% in the zonal average ozone distribution.

4.2.2 Comparison with observations

The Emmons database

A comparison of mean vertical profiles from the flight campaigns collected in the database by Emmons et al. (2000) with the five simulations has been performed. Only campaigns that have been conducted in the same season as the simulation period are used for the analysis. However, since the exact meteorology of the specific years is not reproduced, this analysis has to be considered more qualitatively. For each compound analysed above some profiles are shown in the supplement (<http://www.atmos-chem-phys.net/10/1931/2010/acp-10-1931-2010-supplement.pdf>).

The combined results are shown in the Taylor (2001)-diagram (Fig. 3) depicting normalised standard deviation, correlation and RMS deviation from the measurements. In the corresponding table in the supplement (<http://www.atmos-chem-phys.net/10/1931/2010/acp-10-1931-2010-supplement.pdf>) the biases (model – observations) and the linear regression analysis (for the

method compare Jöckel et al., 2006; Pozzer et al., 2007) are listed. O₃ has been split into “all data” and “data below 9 km altitude”, since in the midlatitudes and polar regions it has been the aim of some of the flights to observe tropopause folds, i.e. stratospheric air in the troposphere, therefore not representing the “typical” tropospheric mixing ratios. Consequently, the normalised standard deviation off all simulations is much better in the “below 9 km” cases than in those including the tropopause region data. None of the campaign data showed an obvious decrease of O₃ concentrations in the upper tropopause due to outflow of convectively transported ozone poor air from the boundary layer. All schemes perform relatively similar, with the EC being slightly superior in terms of correlation and normalised standard deviation; however, the bias (see the table in the supplement <http://www.atmos-chem-phys.net/10/1931/2010/acp-10-1931-2010-supplement.pdf>) is lower than in EC in most of the model simulations except for B1. The tropospheric mixing ratios lie all within the variability of the observations (with a slight high bias for Tasmania), and the strongest deviations occur in the upper troposphere in the extratropics. For the tropical profiles (e.g. TRACE-A, Brazil) the differences between the schemes are bigger, but all are within the observational variability. For H₂O the correlation is very high in all simulations (close to one), but all schemes underestimate the variability (in terms of the normalised standard deviation), the B1 simulation worst. In terms of the linear regression and the bias the agreement is worse: EC with the highest moisture content in the troposphere (see Sect. 4.2.1a) has the lowest bias and the slope that is closest to one, but a very large intercept. The profiles in the supplement (<http://www.atmos-chem-phys.net/10/1931/2010/acp-10-1931-2010-supplement.pdf>) all show a proper agreement with the observations, but there is no data available below 5 km altitude due to the season limitation. HCHO has in all simulations a relatively high correlation (> 0.95), and the variability is captured accurately; only B1 is slightly low. All simulations have a high bias (smallest in T1). Some of the profiles are reproduced relatively well by all schemes, i.e. the model mean is within the standard deviation of the observations, whereas others substantially overestimate the observations. Nevertheless, most of the shape features of the profiles are reproduced, but e.g. the strength of an enhancement at a specific altitude varies from scheme to scheme. The nitric acid distribution is more scattered in terms of the normalised standard deviation, whereas the correlation is ≈0.9 for all simulations. B1 shows the lowest normalised standard deviation, slightly underestimating the variability, but all the others overestimate it (worst for T1). There is almost no bias in EC and a small negative for all the other simulations (worst for Ema). However, the linear regression is best for this scheme, i.e. the slope is closest to one and the intercept is smallest. The vertical profiles are sometimes well reproduced (e.g. TRACE-A, Brazil), but sometimes

substantially overestimate lower tropospheric mixing ratios (e.g. TRACE-A, West African Coast), or underestimate the tropospheric mixing ratios completely (e.g. POLINAT-2, Ireland). Again the schemes behave relatively similarly, such that either the feature is not directly caused by convection or all schemes are able to capture it because of a large-scale forcing causing convection. For CO the correlation is around 0.8 for all simulations and the normalised standard deviation is between 0.6 and 0.8, such that all schemes underestimate the observed variability: EC and B1 perform worse than the other three simulations. For all schemes a negative bias is calculated, and the slope and intercept of the linear regression are relatively similar. For the tropical campaigns, i.e. where convection has the strongest impact, the variability between the schemes is strongest (e.g. TRACE-A, West African Coast). As seen in the global pictures, using B1 leads to enhanced transport into the upper troposphere, but lower mixing ratios at the top of the boundary layer. Additionally, the outflow in T1 appears to be slightly lower, since the CO mixing ratios show a gradient at lower altitude where none of the other schemes produces a similar feature.

From the comparison with the Emmons et al. (2000) database, it is not conclusive which scheme performs best. The simulation using the B1 scheme usually differs a little more strongly from the others, but this is not valid for all compounds.

The GABRIEL campaign

During this campaign, with its measurement period in September and October 2005 (Lelieveld et al., 2008) in Suriname and the Guayanas ten flights with measurements of various trace gases have been performed. For the purpose of comparing the flight data with the model simulations, the tracer mixing ratios are stored every model timestep bilinearly interpolated to the actual position of the aircraft (Jöckel et al., 2010). This online flight tracking requires the position data of the aircraft for the model simulation, but a limitation in time resolution is caused by the length of a model timestep (in this case 10 min).

The mean profiles from this campaign for four exemplary compounds are shown in Fig. 4. For water vapour, all simulations show an underestimation at the surface, at above about 900 hPa, most of the simulations are in the range of the observed values. As in the global picture B1 simulates the driest atmosphere, substantially underestimating water vapour in the lower atmosphere (between 850 and 500 hPa). In contrast to this, EC overestimates moisture also in agreement with the global picture. The Ema simulation is closest to the observations, even though slightly underestimating the observed H₂O, but agreeing best in terms of the shape of the profile.

For CO all simulations fail to capture the observed profiles. Especially, in the lower troposphere the simulated values are underestimated by up to 35%. The strong decrease

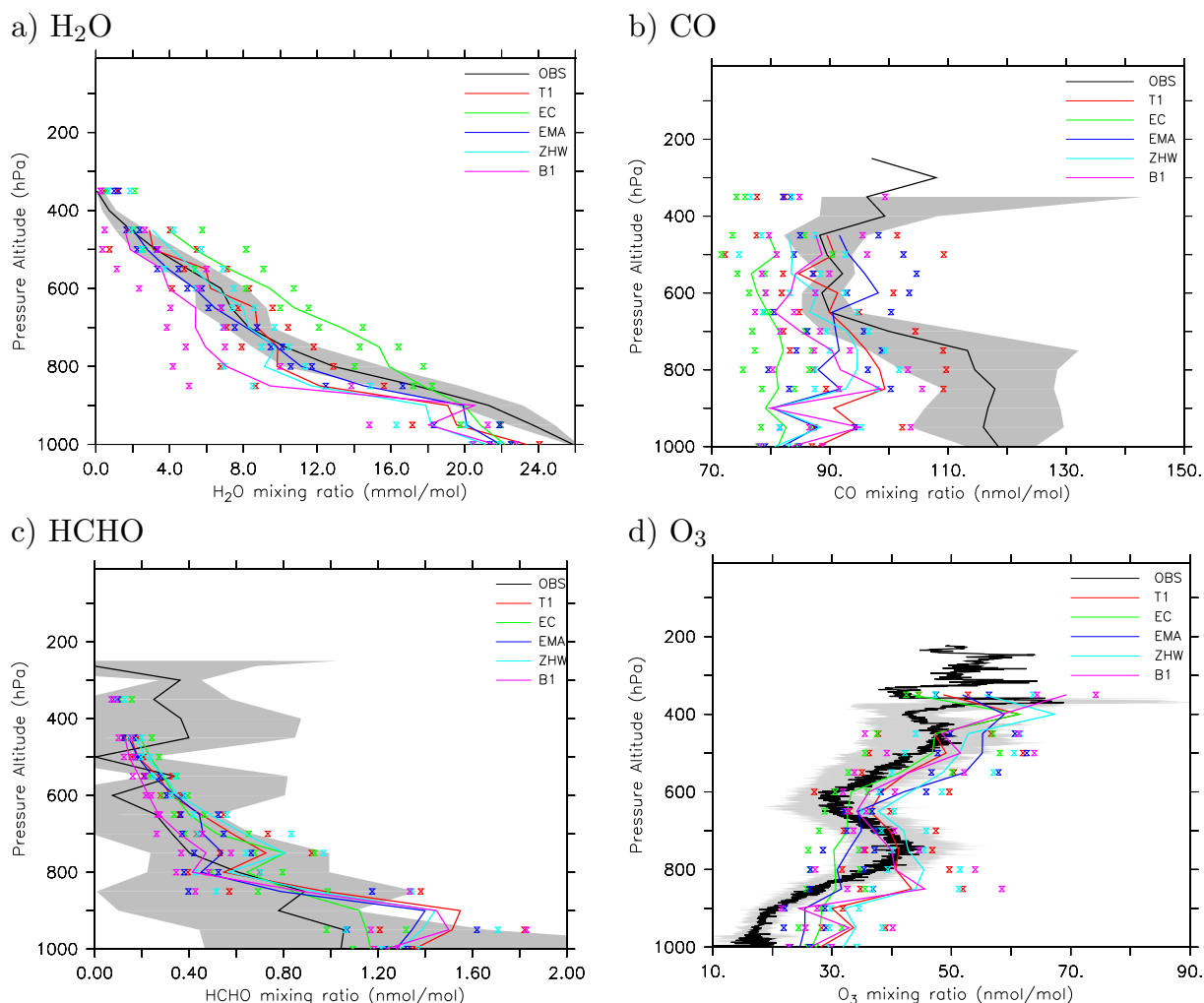


Fig. 4. Average (over all flights) vertical profiles during the GABRIEL campaign. The black line depicts the mean observed profile, grey shaded its standard deviation. The simulations with the different convection schemes are denoted by the colours: red for T1, green for EC, blue for Ema, turquoise for ZHW and magenta for B1. The symbols depict $\pm\sigma$ for the model calculations with respect to time and area.

at the top of the boundary layer is not reproduced by any of the simulations (only indicated in B1), but show a more well mixed profile up to 400 hPa. The mixing ratios above 600 hPa agree better with the observations, especially for Ema, T1 and ZHW. EC values are still underestimated.

In contrast to this, the decrease of mixing ratios with altitude in the formaldehyde profile is captured by all simulations, even though with all schemes the values at the 900 hPa level are enhanced compared to the observations. The enhancement at the 400 hPa level in the observations cannot be properly reproduced by any of the simulations, potentially resulting from convective outflow (either local or transported from within a few hours ago, e.g. the “convective” flight mentioned above).

For O_3 the shape of the profile is overall reproduced; however either some of the enhancements and lower mixing ratios are not captured with the correct value or the increase

towards the upper troposphere is too strong. For instance EC reproduces the mixing ratios above 600 hPa almost perfectly, but the ozone below is almost completely mixed, not following the observed profile. Almost all the other schemes show an enhancement below 800 hPa which is lower than the observed one at ≈ 750 hPa, and a minimum at around 600 hPa which is also observed. Ema is slightly high in the upper troposphere, and all the other schemes are in the range of 1σ of the observations. In agreement with the moisture and also the OH underestimation (see Lelieveld et al., 2008) surface O_3 levels are overestimated for all simulations.

The correlation values for simulated compounds compared to the measurements are listed in the supplement (<http://www.atmos-chem-phys.net/10/1931/2010/acp-10-1931-2010-supplement.pdf>). Some of the values are relatively low, showing no good agreement between the simulations and the observations. Combining the analysis

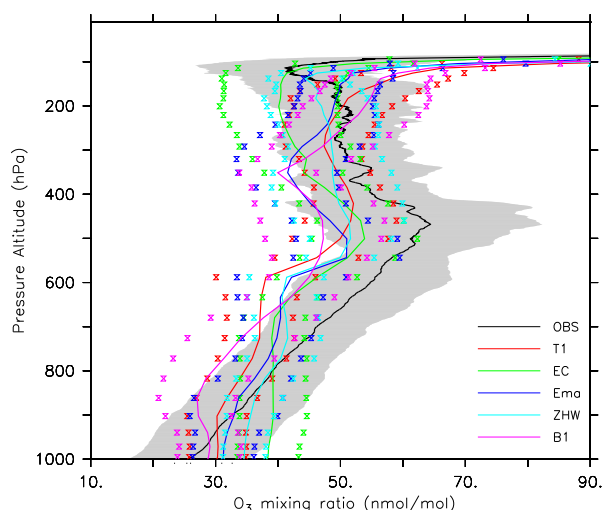


Fig. 5. Vertical profiles from the O₃ sondes launched at Darwin during the SCOUT-O3/ACTIVE campaign. The black line depicts the mean observed profile, grey shaded its standard deviation. The simulations with the different convection schemes are denoted by the colours: red for T1, green for EC, blue for Ema, turquoise for ZHW and magenta for B1. The symbols depict $\pm\sigma$ for the model calculations with respect to time and area.

from both, the profiles and the correlation, the Ema simulation seems generally to be best suited for this campaign. However, for a specific compound in a specific region, e.g. O₃ above 500 hPa other schemes are superior to the overall “best” one.

One of the reasons for the disagreement is the triggering of convection in the simulations at places where in reality no convective event has been observed or vice versa. Consequently, simulated and measured meteorological conditions do not necessarily match, even though the “nudging” technique towards the analysed meteorology has been applied; however, convection and the convective parameterisation are not directly affected by the “nudging” which is a synoptic scale forcing, but react to the simulated meteorology and feedback on the synoptic scale variables. For the “convective” flight of the GABRIEL campaign an additional analysis showed that the convective activity on this particular day differed substantially between the simulations, and only one scheme has captured a deep convective event within a 400 km distance from the flight track. Synoptic scale forced convection, e.g. frontal or conveyor belt convection is, however, triggered by all schemes at similar locations.

The SCOUT-O3/ACTIVE Darwin campaign

From this campaign much more data is available than from GABRIEL, since four aircraft have been used observing at various altitudes simultaneously, in addition to O₃ sondes providing more vertical profile data. For more information,

a campaign and objective description, measurement techniques, etc. we refer to Vaughan et al. (2008). Furthermore, this campaign has been designed to analyse the impact of convection. However, the convective system “Hector” is a subgrid-scale feature for the global model with the current resolution that it is not resolved explicitly and hence not forced by the “nudging” technique. Therefore, similar limitations as for the GABRIEL campaign have to be considered.

a) Ozone sondes:

The O₃ sondes launched daily from Darwin during the campaign days have been compared with the ozone mixing ratios from the five different simulations. The average profile depicted in Fig. 5 shows lowest values at the surface, increasing values to 480 hPa, then a decrease up to 200 hPa and a characteristic minimum slightly below 100 hPa. The maximum has been identified as the influence of stratospheric air during Rossby wave breaking events (Vaughan et al., 2008). The minimum at ≈ 100 hPa agrees well with the typical convective storm height, representing the convective outflow of low O₃ containing air from the boundary layer. All of the simulations have significant problems in reproducing the ozone values in the lower troposphere, independent of the convection scheme: surface mixing ratios are higher than observed (mostly within the grey shaded 1σ range), but for most of the schemes (all, except B1 which captures the slope but has a low bias) the gradient is not as steep as in the observations. With all convection parameterisations a local maximum between 520 and 420 hPa is simulated, with EC and ZHW being able to reproduce the altitude almost perfectly, but all schemes underestimate the observed values (B1 is even outside the 1σ range). However, the upper tropospheric minimum representing the convective outflow of O₃ poor air from low altitudes is not captured at the correct altitude by B1 and Ema (350 hPa). Also the outflow of T1 is much too low, peaking slightly above 300 hPa. Only EC and ZHW are able to reproduce low ozone values up to almost 100 hPa (with EC being slightly low biased) and the subsequent steep gradient towards the stratospheric ozone levels. Further upwards, the ozone levels are simulated accurately independent of the choice of the convection scheme. The corresponding tropospheric correlations (calculated from the surface to the 100 hPa level, without the error correction applied for in Sect. 4.2.2.1) are $R^2 = 0.39$ for T1, 0.64 for EC, 0.52 for Ema, 0.57 for ZHW and 0.42 for B1.

Overall, with none of the schemes a perfect reproduction of the observed O₃ profiles can be achieved: B1 has the best lower to mid-tropospheric shape, EC and ZHW are best for the upper tropospheric part, but almost all simulations are within the 1σ range of the observations. The variability of the model simulations is of similar magnitude as the observed one. Since EC has the best correlation and some good shape properties of the observed profile can be reproduced, it should be considered most adequate for this comparison.

b) Flight profiles:

Figure 6 shows an overview of the averaged vertical profiles as observed during the SCOUT-O3/ACTIVE campaign and the corresponding model results. In contrast to Palazzi et al. (2009) this study focuses more on tropospheric data. As for the section above, the black line depicts the measurements (with the grey shaded area representing the $\pm 1\sigma$ range) and the coloured lines the model simulations using the different convection schemes.

For water vapour the observed profiles (see Schiller et al., 2009) are captured in good agreement with the observations¹¹. For the Geophysica data (from the FISH (Fast In-situ Stratospheric Hygrometer) instrument only, Fig. 6a), the values show only little variability in the uppermost troposphere and lower stratosphere, such that the small overestimation by Ema and ZHW is larger than 1σ . While B1 and EC (this one even stronger) underestimate H_2O in the low altitude range of the observations (at 350 hPa), all other simulations overestimate the UTLS moisture; none of them capture some of the extremely low observed values at this altitude. Nevertheless the correlation is very high (almost unity) for all simulations. For the data from the Falcon flights (Fig. 6b), also using a FISH instrument, the variation between the simulations is more obvious. T1, Ema and B1 follow the observations well in the lower troposphere, whereas EC underestimates the values below 750 hPa, but overestimates above up to 500 hPa. Between 600 and 250 hPa all other simulations overestimate water vapour from these measurements by $\approx 1\sigma$. The behaviour of EC agrees well with the global picture below the 500 hPa level. In contrast to this, the B1 simulation is not drier than observed as expected from the global behaviour. The overall agreement makes it difficult to judge a “best” performance with the correlation being almost unity again. The bias is lowest in the B1 for the Geophysica and in the Ema simulation for the Falcon data.

Upper tropospheric SO_2 (Fig. 6c) is completely underestimated (by one order of magnitude) by all simulations. The elevated levels of sulphur dioxide at 800 hPa are not captured with any scheme, and above the conversion to sulphate and wet deposition lead to a stronger removal of gaseous SO_2 in the simulations than the observations on-board the Falcon suggest. However, the levels of SO_2 are relatively low, such that this air mass is almost unpolluted. The B1 and Ema simulation perform “best” in terms of correlation and bias.

CO depicted in Fig. 6d-f has been observed from three of the aircrafts with focus on various altitude levels due to the mission concept: the Geophysica measured above the convection using a COLD instrument (Viciani et al., 2008), the Egrett in the convective outflow level and the Dornier at the convective inflow and lower troposphere. All simulations substantially underestimate the low altitude carbon monoxide which might be caused by underestimated emissions.

¹¹Note the logarithmic scale in the graphs for H_2O .

This agrees with the results from the GABRIEL campaign. However, for this case EC, Ema and ZHW have the higher values (being at least in the 1σ -range of the Dornier data, and not T1 and B1 (which had this for GABRIEL)). For the middle troposphere, the Ema and ZHW simulation show a similar slope as the Egrett data, whereas B1 is almost completely well mixed in the whole troposphere and T1 and also EC show a weaker gradient between convective in- and outflow. The UTLS values of the Geophysica are only captured at the transition into the stratosphere. None of the schemes performs extraordinary well: best performance in terms of correlation and bias shows B1 for the Geophysica and ZHW for the Egrett data. For the Dornier, some of the simulations are even anti-correlated to the observations.

Analysing the O_3 profiles (see Fig. 6g-h) from the Geophysica using a FOZAN instrument (Ulanovsky et al., 2001) a similar shape and behaviour as for the ozone sondes (Sect.4.2.2.3a) is found. All simulations mainly follow the observations, but the upper tropospheric minimum is only captured by EC and ZHW. Lower tropospheric values are overestimated for both the Geophysica and the Dornier data. However, the Dornier data shows a substantially weaker vertical gradient than the sondes and the Geophysica. This is also not simulated with any of the convection parameterisations, causing the overestimation of the simulation data compared with these measurements. For the Geophysica data T1 performs “best” in terms of the bias, but EC in terms of the shape of the profile (highest correlation), T1 also has the lowest bias for the Dornier data.

The NO data from the Falcon is in general much higher than the simulated values, but show a very large variability. Due to NO_x production by lightning during the convective events a perfect match of simulated and observed convection and associated lightning NO_x emissions would be required. The analysis of triggered convective events compared to the observed Hector appearances shows that the global model does not always capture the development of strong convection in that region. Therefore it is very difficult to achieve a good agreement of short-lived compounds which are more susceptible to the influence of convection with any of the applied parameterisation schemes. Even though there is usually convective activity simulated on most of the flight days, it is hardly correlated with the observed one. Therefore, only the impact of convection on the longer lived species can be reproduced well (e.g. O_3 and upper tropospheric CO).

4.3 Scavenging and wet deposition

The different convection schemes not only cause different precipitation patterns (see Tost et al., 2006b and <http://www.atmos-chem-phys.net/10/1931/2010/acp-10-1931-2010-supplement.pdf>), but also result in different vertical distributions of cloud and precipitable water. Consequently, the scavenging efficiency for trace gases and aerosols depends not only on the distribution of

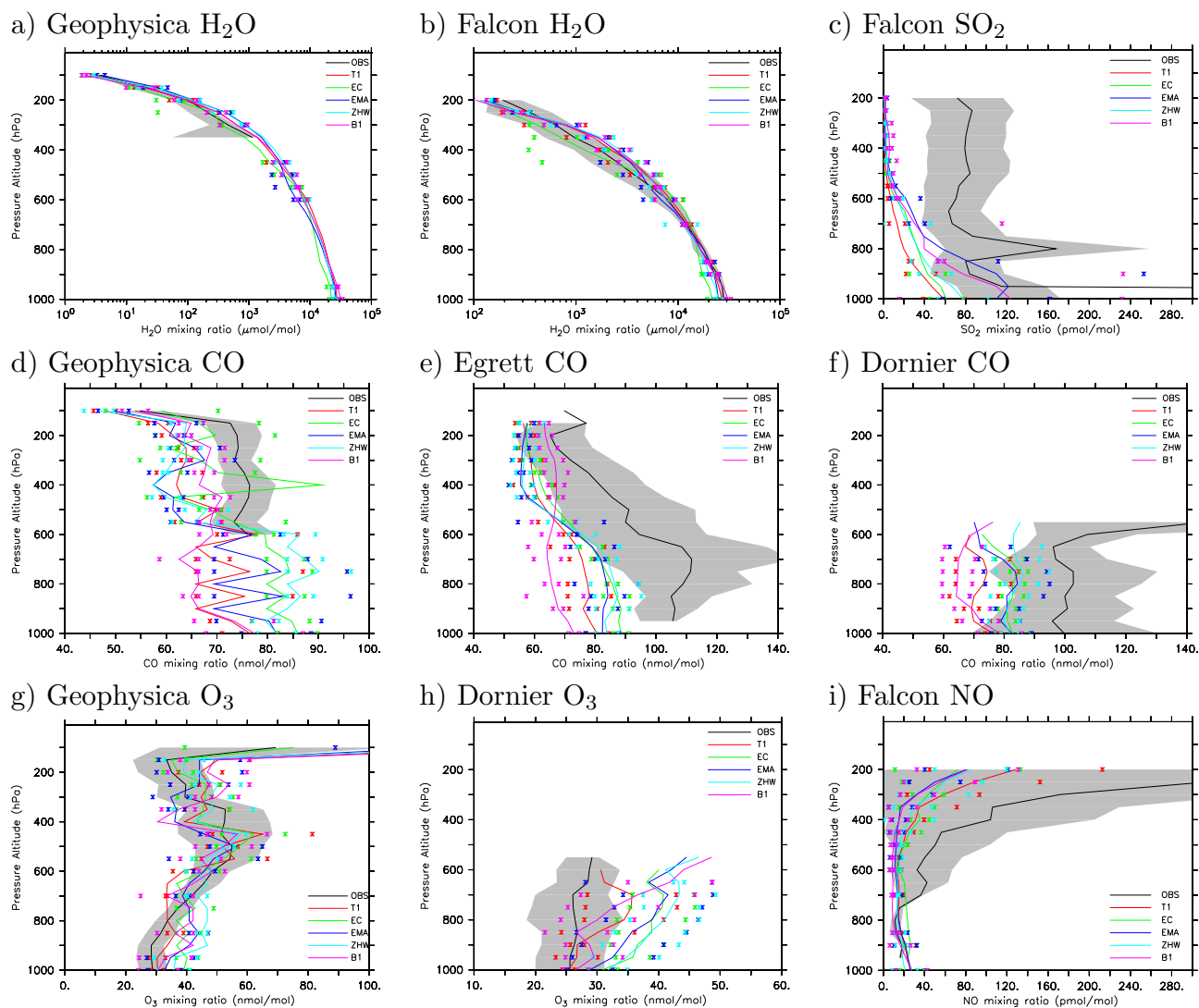


Fig. 6. Average (over all flights) vertical profiles from the various aircraft during SCOUT-O3/ACTIVE starting from Darwin. The black line depicts the mean observed profile, grey shaded its standard deviation. The simulations with the different convection schemes are denoted by the colours: red for T1, green for EC, blue for Ema, turquoise for ZHW and magenta for B1. The symbols depict $\pm\sigma$ for the model calculations with respect to time and area.

the species (due to the convective transport), but also on the condensed water and the precipitation regions. However, since the global precipitation distribution differs only within the range of uncertainty by Tost et al. (2006b), the overall wet deposition looks relatively similar in all simulations. Nevertheless some differences are evident.

Figure 7 depicts the differences in the zonal averages of the accumulated wet deposition of the two main acidifying compounds nitrate and sulphate. The general features are very similar (except for NO_3^- in ZHW), and are mainly caused by the climatologically correct occurrence of precipitation and subsequent wet deposition. The total amount differs according to differences in the precipitation, e.g., since ZHW forms usually less precipitation over the

oceans, the total amount of wet deposition is lower. Detailed pictures of the location of the main differences are part of the supplement (<http://www.atmos-chem-phys.net/10/1931/2010/acp-10-1931-2010-supplement.pdf>). Nevertheless, stronger wet deposition does not necessarily mean lower atmospheric burden, since enhanced wet deposition can be compensated by reduced dry deposition and vice versa. The relative differences in the wet deposition are smaller than those in the tracer distributions since strong convective activity is characterised by both, strong upward motion (vertical tracer transport) and strong precipitation (resulting in strong wet deposition). Consequently, for highly soluble compounds like nitrate the strong upward motion is largely compensated by the downward motion within the

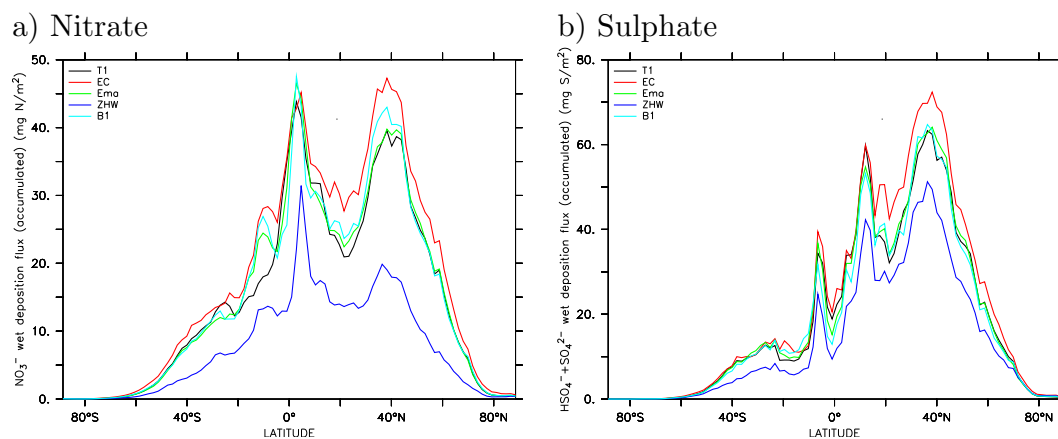


Fig. 7. Accumulated zonally averaged nitrate (a) and sulphate (b) wet deposition flux (each in mg N or S per m²) at the surface. The different colours denote the different simulations.

precipitation. Additionally, if the convective precipitation is not occurring in one specific grid box, convective activity likely occurs one time step later or in the adjacent grid box. Alternatively the precipitation is formed by the large-scale cloud scheme. Consequently, lower wet removal by convective precipitation is balanced by stronger wet removal by large-scale precipitation, perhaps with only a slight shift in the patterns. For sulphate wet deposition the differences in liquid water cause different in-cloud sulphate production which is also affected by the different oxidant distributions. Consequently, the combined effects on chemistry and cloud processes cause slightly larger differences locally. On the other hand, for sulphate the source (i.e., the in-cloud sulphate formation) is more directly linked to the sink by wet deposition. Therefore, the zonal average distribution of SO₄²⁻ shows smaller differences for the ZHW scheme than for nitrate, since via cloud and precipitation formation both the source and the sink processes take place simultaneously. Additionally, the sulphate production from the anthropogenic SO₂ emissions are mostly located in regions where large-scale precipitation is as important as convective, in contrast to nitrate, which has substantial emissions in the tropical regions from biomass burning, soil emissions and lightning.

In comparison to the observation data used by Tost et al. (2007a) the EC simulation agrees better in terms of correlation and linear fit than the T1 simulation for both NO₃⁻ and SO₄²⁻. For sulphate all other simulations show a higher correlation than T1 for the selected stations. Further details can be found in the supplement (<http://www.atmos-chem-phys.net/10/1931/2010/acp-10-1931-2010-supplement.pdf>).

5 Discussion

One additional source of uncertainty is the “tuning” of the model setups: Depending on the choice of the convection scheme, several parameters in the model setup can be used

to “tune” the radiation balance (and also the precipitation) to achieve an agreement with observations. In this study, this tuning was applied within the convection parameterisation in terms of the convective relaxation time and the convective precipitation formation rate (i.e., the conversion rate of convective cloud water into precipitation). Additionally, the entrainment and detrainment rates for the individual convection schemes are selected in agreement with recommendations from their authors. This partly explains why the convective mass fluxes and consequently the tracer distributions show such a strong dependence on the selected convection scheme.

Since the conversion of cloud water to precipitation not only determines the total rainfall, but also the energy budget within the cloud, the temperature profiles are affected, e.g. the more cloud water is transformed into precipitation that falls out of the cloud immediately, the less energy is required to evaporate the rest of the cloud (i.e., the evaporative cooling is smaller). Furthermore, decreasing the amount of condensed water by removal in the form of precipitation decreases the moist static energy, and consequently stabilises the atmosphere. Both of these stabilising effects consequently further decrease convective activity.

Entrainment and detrainment rates are crucial for the strength of the mass fluxes, since an overestimated entrainment causes a large mass of air to be lifted, but decreases the buoyancy compared to the surroundings, consequently preventing very deep convection. A weak entrainment allows deeper convection, but only with a relatively small total amount of air moved, resulting in weak mixing in the global model column. Detrainment must be considered as well: a strong detrainment in the mid troposphere prevents very deep convection and vice versa. However, even though a large degree of freedom for these processes exists; for instance Ott et al. (2008) showed that using different parameters in the entrainment and detrainment calculation of one convection

scheme climatologically realistic fields for radiation, precipitation, moisture and temperature can be achieved. The same holds for the treatment of tracer transport, e.g., a bulk versus a plume ensemble transport formulation (Lawrence and Rasch, 2005), justifying such a study.

Since the overall effects of deep convection and the differences between the simulations are relatively large, the question of how to proceed on this issue arises. However, due to the complexity of the system a traceback to the original causes for each individual difference is difficult, and can only be attempted by the analysis of different compounds with various characteristics such as chemical reactivity and lifetime, solubility, and source distribution. A potential solution for the detailed process analysis would be a comparable study in a single column model under well defined prescribed input/boundary conditions, e.g. an extension of the study of Mahowald et al. (1995) using a comprehensive chemical reaction system in multiple phases. Nevertheless, some parts of the parameterisations are quite complex by themselves, e.g., convective microphysics, so that even in such a study a variety of results that are difficult to interpret is likely. Since in the global atmosphere a large variety of possible atmospheric conditions occur, which can be represented only by a huge set of convective single column models, global modelling studies are much better suited to capture all of these features, especially if the interaction of convection dynamics and the feedback on the synoptic scale should be considered.

Since computer models of the atmospheric chemistry are usually highly non-linear (diffusion, chemistry, feedbacks, sink processes), very small deviations between simulations can easily be enhanced by the model equations resulting in larger differences. Therefore, some of the differences analysed in the sections above, e.g., those in the range of $\approx 5\%$, are not necessarily caused by the different convection schemes, but by these non-linearities. However, for some compounds a much larger variation dependent on the convection scheme has been detected, which cannot be attributed alone to these causes. Furthermore, since all model simulations have been nudged towards the ECMWF reanalysis, the differences in the synoptic scale weather phenomena are small.

One important aspect to point out is that it is not the main intention of this study to rate the schemes according to their performance, but to quantify the uncertainty resulting from the physical parameterisations (in our case moist convection) in an atmospheric chemistry GCM. Depending on the species under investigation and the region some schemes perform better or worse. The triggering of convective activity in a global model at the observed location seems to be very difficult, if the convection is not forced by large-scale meteorological conditions. For more local convection this appears to be more randomly distributed depending on the choice of the convection scheme.

Due to compensating errors/uncertainties and non-linearities not all of the effects can be easily transferred from one compound or one cause or also one model to the next. Additionally, not all of the cause-effect relationships can be readily revealed.

6 Conclusions

In this study, it has been shown that the choice of the convection parameterisation in a global model of the chemical composition of the atmosphere has a substantial influence on trace gas distributions. Five different state-of-the-art convection schemes have been used in an atmospheric chemistry GCM (“nudged” by the same large-scale meteorology) and the resulting trace gas distributions have been compared. The main goal is to quantify the uncertainty for the process of parameterised convection on trace gases. The comparison with observations from various sources shows that none of the schemes is extremely different from the others, and all have advantages and disadvantages in reproducing observed tracer distributions. Depending on the atmospheric lifetime and the relevant processes for a specific compound, the averaged differences can be up to $\pm 100\%$. For O_3 and CO the maximum uncertainty is globally less than $\pm 25\%$, but even for these gases differences can locally exceed a $\pm 100\%$.

The reasons for the differences are to be found both, in meteorology, i.e., varying intensity and frequency of convective events, and in chemistry, i.e., precursors are affected differently by the convection due to solubility, reaction partners and location where the chemical reactions take place. Chemical and meteorological effects cannot be easily separated, so the only way to address meteorological effects alone is by using chemically inactive tracers such as ^{222}Rn . An additional important meteorological effect determined by the convection scheme is the formation of cloud and rain water and subsequent redistribution and removal of constituents from the atmosphere by precipitation scavenging. This is of larger importance for soluble compounds, but can also have a substantial effect on other species due to precursor interactions and removal. The role of water vapour as source for OH is also relevant, since higher moisture affects the oxidation capacity of the atmosphere and consequently has an influence on almost all chemical compounds. Overall, convection parameterisations are a large source of uncertainty, as well known in the community; in this study we have made an important step towards characterising and quantifying these uncertainties.

Acknowledgements. We thank J. Lelieveld for the support in performing this study, and A. Pozzer for some of the scripts for data analysis. We wish to acknowledge the use of the Ferret program for analysis and graphics in this paper. Ferret is a product of NOAA’s Pacific Marine Environmental Laboratory. (Information is available at <http://ferret.pmel.noaa.gov/Ferret/>). We thank the NERC for funding the ACTIVE project and to the NERC ARSF facility for

operating the Dornier during ACTIVE as well as the integrated European project SCOUT-O3. Furthermore, we thank the DKRZ for their support and the possibility to perform the calculations on computing devices maintained by this institution. Additionally we thank all MESSy developers and users for their support, hints, proposals and discussions. This work has been partly performed within the ENIGMA project, funded by the Max Planck society. The GABRIEL-Team are: J. Lelieveld, H. Fischer, H. Harder, M. Martinez-Harder, J. Williams, B. Scheeren, R. Maser, C. Becker, D. Rodriguez, B. Tan, G. Wesenhagen, H. Bozem, C. Gurk, U. Parchatka, C. L. Schiller, R. Königstedt, A. Stickler, G. Eerdeken, N. Yassaa, V. Sinha, S. Gebhardt, R. Hofmann, T. Klüpfel, A. Coulomb, S. Bartenbach, D. Kubistin. The SCOUT-O3-Darwin/ACTIVE Team PIs are G. Vaughan, A. Volz-Thomas, A. Lewis, J. Lee, F. Ravagnani, A. Ulanovski, C. Schiller, S. Viciani, F. d'Amato, H. Schlager, A. Giez, G. Shur, D. Davis, J. Hacker, A. Heymsfield, M. Gallagher, R. Busen, J. Whiteway, S. Borrmann and many more, who contributed to the successful campaign achievements.

The service charges for this open access publication have been covered by the Max Planck Society.

Edited by: M. Dameris

References

- Arakawa, A.: The Cumulus Parameterization Problem: Past, Present, and Future, *J. Clim.*, 17, 2493–2525, 2004.
- Arakawa, A. and Schubert, W. H.: Interaction of a Cumulus Cloud Ensemble with the Large-Scale Environment, Part I, *J. Atmos. Sci.*, 31, 674–701, 1974.
- Bechtold, P., Bazile, E., Guichard, F., Mascart, P., and Richard, E.: A mass-flux convection scheme for regional and global models, *Q. J. R. Meteorol. Soc.*, 127, 869–886, 2001.
- Bechtold, P., Chaboureaud, J.-P., Beljaars, A., Betts, A. K., Köhler, M., Miller, M., and Redelsperger, J.-L.: The simulation of the diurnal cycle of convective precipitation over land in a global model, *Q. J. R. Meteorol. Soc.*, 130, 3119–3137, 2004.
- Brunner, D., Siegmund, P., May, P. T., Chappel, L., Schiller, C., Mller, R., Peter, T., Fueglistaler, S., MacKenzie, A. R., Fix, A., Schlager, H., Allen, G., Fjaeraa, A. M., Streibel, M., and Harris, N. R. P.: The SCOUT-O3 Darwin Aircraft Campaign: rationale and meteorology, *Atmos. Chem. Phys.*, 9, 93–117, 2009, <http://www.atmos-chem-phys.net/9/93/2009/>.
- Doherty, R. M., Stevenson, D. S., Collins, W. J., and Sanderson, M. G.: Influence of convective transport on tropospheric ozone and its precursors in a chemistry-climate model, *Atmos. Chem. Phys.*, 5, 3205–3218, 2005, <http://www.atmos-chem-phys.net/5/3205/2005/>.
- Donner, L. J., Seman, C. J., Hemler, R. S., and Fan, S.: A Cumulus Parameterization Including Mass Fluxes, Convective Vertical Velocities, and Mesoscale Effects: Thermodynamic and Hydrological Aspects in a General Circulation Model, *J. Clim.*, 14, 3444–3463, 2001.
- Emanuel, K. A. and Zivkovic-Rothman, M.: Development and Evaluation of a Convection Scheme for Use in Climate Models, *J. Atmos. Sci.*, 56, 1766–1782, 1999.
- Emmons, L. K., Hauglustaine, D. A., Müller, J.-F., carroll, M. A., Brasseur, G. P., Brunner, D., Staehelin, J., Thouret, V., and Marengo, A.: Data composites of airborne observations of tropospheric ozone and its precursors, *J. Geophys. Res.*, 105, 20497–20538, 2000.
- Hack, J. J.: Parameterization of moist convection in the National Center for Atmospheric Research community climate model (CCM2), *J. Geophys. Res.*, 99, 5551–5568, 1994.
- Jacob, D. J. and Prather, M. J.: Radon-222 as a test of convective transport in a general circulation model, *Tellus*, 42B, 118–134, 1990.
- Jöckel, P.: Technical Note: Recursive discretisation of geoscientific data in multiple dimensions in the Modular Earth Submodel System (MESSy) data import interface, *Atmos. Chem. Phys.*, 6, 3557–3562, 2006, <http://www.atmos-chem-phys.net/6/3557/2006/>.
- Jöckel, P., Sander, R., Kerkweg, A., Tost, H., and Lelieveld, J.: Technical Note: The Modular Earth Submodel System (MESSy) – a new approach towards Earth System Modeling, *Atmos. Chem. Phys.*, 5, 433–444, 2005, <http://www.atmos-chem-phys.net/5/433/2005/>.
- Jöckel, P., Tost, H., Pozzer, A., Brühl, C., Buchholz, J., Ganzeveld, L., Hoor, P., Kerkweg, A., Lawrence, M. G., Sander, R., Steil, B., Stiller, G., Tanarhte, M., Taraborrelli, D., van Aardenne, J., and Lelieveld, J.: The atmospheric chemistry general circulation model ECHAM5/MESSy1: consistent simulation of ozone from the surface to the mesosphere, *Atmos. Chem. Phys.*, 6, 5067–5104, 2006, <http://www.atmos-chem-phys.net/6/5067/2006/>.
- Jöckel, P., Kerkweg, A., Buchholz-Dietsch, J., Tost, H., Sander, R., and Pozzer, A.: Technical Note: Coupling of chemical processes with the Modular Earth Submodel System (MESSy) submodel TRACER, *Atmos. Chem. Phys.*, 8, 1677–1687, 2008, <http://www.atmos-chem-phys.net/8/1677/2008/>.
- Kerkweg, A., Buchholz, J., Ganzeveld, L., Pozzer, A., Tost, H., and Jöckel, P.: Technical Note: An implementation of the dry removal processes DRY DEPosition and SEDimentation in the Modular Earth Submodel System (MESSy), *Atmos. Chem. Phys.*, 6, 4617–4632, 2006a.
- Kerkweg, A., Sander, R., Tost, H., and Jöckel, P.: Technical Note: Implementation of prescribed (OFFLEM), calculated (ONLEM), and pseudo-emissions (TNUDGE) of chemical species in the Modular Earth Submodel System (MESSy), *Atmos. Chem. Phys.*, 6, 3603–3609, 2006b.
- Kerkweg, A., Jöckel, P., Pozzer, A., Tost, H., Sander, R., Schulz, M., Stier, P., Vignati, E., Wilson, J., and Lelieveld, J.: Consistent simulation of bromine chemistry from the marine boundary layer to the stratosphere, Part I: model description, sea salt aerosols and pH, *Atmos. Chem. Phys.*, 8, 5899–5917, 2008, <http://www.atmos-chem-phys.net/8/5899/2008/>.
- Kuo, H. L.: Further Studies of the Parameterization of the Influence of Cumulus Convection on Large-Scale Flow, *J. Atmos. Sci.*, 31, 1232–1240, 1974.
- Lawrence, M. G. and Rasch, P. J.: Tracer transport in deep convective updrafts: plume ensemble versus bulk formulations, *J. Atmos. Sci.*, 62, 2880–2894, 2005.
- Lawrence, M. G. and Salzmann, M.: On interpreting studies of tracer transport by deep cumulus convection and its effects on atmospheric chemistry, *Atmos. Chem. Phys.*, 8, 6037–6050, 2008.

- <http://www.atmos-chem-phys.net/8/6037/2008/>.
- Lawrence, M. G., v. Kuhlmann, R., Salzmann, M., and Rasch, P. J.: The balance of effects of deep convective mixing on tropospheric ozone, *Geophys. Res. Lett.*, 30, 1940, doi:10.129/2003GL017644, 2003.
- Lelieveld, J. and Crutzen, P. J.: Role of Deep Cloud convection in the Ozone Budget of the Troposphere, *Science*, 264, 1759–1761, 1994.
- Lelieveld, J., Brühl, C., Jöckel, P., Steil, B., Crutzen, P. J., Fischer, H., Giorgetta, M. A., Hoor, P., Lawrence, M. G., Sausen, R., and Tost, H.: Stratospheric dryness: model simulations and satellite observations, *Atmos. Chem. Phys.*, 7, 1313–1332, 2007, <http://www.atmos-chem-phys.net/7/1313/2007/>.
- Lelieveld, J., Butler, T. M., Crowley, J. N., Dillon, T. J., Fischer, H., Ganzeveld, L., Harder, H., Lawrence, M. G., Martinez, M., Taraborrelli, D., and Williams, J.: Atmospheric oxidation capacity sustained by a tropical forest, *Nature*, 452, 737–740, 2008.
- Lin, J. W.-B. and Neelin, J. D.: Considerations for Stochastic Convective Parameterization, *J. Atmos. Sci.*, 59, 959–975, 2002.
- Lohmann, U. and Roeckner, E.: Design and performance of a new cloud microphysics scheme developed for the ECHAM general circulation model, *Climate Dynam.*, 12, 557–572, 1996.
- Mahowald, N. M., Rasch, P. J., and Prinn, R. G.: Cumulus parameterizations in chemical transport models, *J. Geophys. Res.*, 100, 26173–26189, 1995.
- Mahowald, N. M., Rasch, P. J., Eaton, B. E., Whittlestone, S., and Prinn, R. G.: Transport of ²²²Rn to the remote troposphere using the Modell of Atmospheric Transport and Chemistry and assimilated winds from ECMWF and the National Center for Environmental Prediction/NCAR, *J. Geophys. Res.*, 102, 28139–28151, 1997.
- Nober, F. J. and Graf, H. F.: A new convective cloud field model based on principles of self-organisation, *Atmos. Chem. Phys.*, 5, 2749–2759, 2005, <http://www.atmos-chem-phys.net/5/2749/2005/>.
- Nordeng, T. E.: Extended versions of the convective parametrization scheme at ECMWF and their impact on the mean and transient activity of the model in the tropics, *Tech. Rep.* 206, ECWMF, 1994.
- Ott, L., Pawson, S., and Bacmeister, J.: Quantifying the role of convection and other transport processes in determining CO distribution in the free troposphere, in: IGAC conference, 2008.
- Palazzi, E., Fierli, F., Cairo, F., Cagnazzo, C., Donfrancesco, G. D., Manzini, E., Ravagnani, F., Schiller, C., D'Amato, F., and Volk, C. M.: Diagnostics of the Tropical Tropopause Layer from in-situ observations and CCM data, *Atmos. Chem. Phys.*, 9, 9349–9367, 2009, <http://www.atmos-chem-phys.net/9/9349/2009/>.
- Pozzer, A., Jöckel, P., Sander, R., Williams, J., Ganzeveld, L., and Lelieveld, J.: Technical Note: The MESSy-submodel AIRSEA calculating the air-sea exchange of chemical species, *Atmos. Chem. Phys.*, 6, 5435–5444, 2006, <http://www.atmos-chem-phys.net/6/5435/2006/>.
- Pozzer, A., Jöckel, P., Tost, H., Sander, R., Ganzeveld, L., Kerkweg, A., and Lelieveld, J.: Simulating organic species with the global atmospheric chemistry general circulation model ECHAM5/MESSy1: a comparison of model results with observations, *Atmos. Chem. Phys.*, 7, 2527–2550, 2007, <http://www.atmos-chem-phys.net/7/2527/2007/>.
- Price, C., Penner, J., and Prather, M.: NO_x from lightning, 1. Global distribution based on lightning physics, *J. Geophys. Res.*, 102, 5929–5941, 1997.
- Roeckner, E., Bäuml, G., Bonaventura, L., Brokopf, R., Esch, M., Giorgetta, M., Hagemann, S., Kirchner, I., Kornblüeh, L., Manzini, E., Rhodin, A., Schleese, U., Schulzweida, U., and Tompkins, A.: The atmospheric general circulation model ECHAM5: Part 1, *Tech. Rep.* 349, Max-Planck-Institut für Meteorologie, 2003.
- Roeckner, E., Brokopf, R., Esch, M., Giorgetta, M., Hagemann, S., Kornblüeh, L., Manzini, E., Schleese, U., and Schulzweida, U.: Sensitivity of simulated climate to horizontal and vertical resolution in the ECHAM5 atmosphere model, *J. Clim.*, 19, 3771–3791, 2006.
- Sander, R., Kerkweg, A., Jöckel, P., and Lelieveld, J.: Technical Note: The new comprehensive atmospheric chemistry module MECCA, *Atmos. Chem. Phys.*, 5, 445–450, 2005, <http://www.atmos-chem-phys.net/5/445/2005/>.
- Schiller, C., Groöß, J.-U., Konopka, P., Pläger, F., Silva dos Santos, F. H., and Spelten, N.: Hydration and dehydration at the tropical tropopause, *Atmos. Chem. Phys.*, 9, 9647–9660, 2009, <http://www.atmos-chem-phys.net/9/9647/2009/>.
- Tabazadeh, A., Toon, O. B., and Jensen, E. J.: A surface chemistry model for nonreactive trace gas adsorption on ice: Implications for nitric acid scavenging by cirrus, *Geophys. Res. Lett.*, 26, 2211–2214, 1999.
- Taylor, K. E.: Summarizing multiple aspects of model performance in a single diagram, *J. Geophys. Res.*, 106, 7183–7192, 2001.
- Tiedtke, M.: A Comprehensive Mass Flux Scheme for Cumulus Parametrization in Large-Scale Models, *Mon. Weather Rev.*, 117, 1779–1800, 1989.
- Tost, H.: Global Modelling of Cloud, Convection and Precipitation Influences on Trace Gases and Aerosols, Ph.D. thesis, Rheinische Friedrich-Wilhelms-Universität Bonn, Germany, available at: http://hss.ulb.uni-bonn.de/diss_online/math_nat_fak/2006/tost_holger, 2006.
- Tost, H., Jöckel, P., Kerkweg, A., Sander, R., and Lelieveld, J.: Technical Note: A new comprehensive SCAVenging submodel for global atmospheric chemistry modelling, *Atmos. Chem. Phys.*, 6, 565–574, 2006a, <http://www.atmos-chem-phys.net/6/565/2006/>.
- Tost, H., Jöckel, P., and Lelieveld, J.: Influence of different convection parameterisations in a GCM, *Atmos. Chem. Phys.*, 6, 5475–5493, 2006b, <http://www.atmos-chem-phys.net/6/5475/2006/>.
- Tost, H., Jöckel, P., Kerkweg, A., Pozzer, A., Sander, R., and Lelieveld, J.: Global cloud and precipitation chemistry and wet deposition: tropospheric model simulations with ECHAM5/MESSy1, *Atmos. Chem. Phys.*, 7, 2733–2757, 2007a, <http://www.atmos-chem-phys.net/7/2733/2007/>.
- Tost, H., Jöckel, P., and Lelieveld, J.: Lightning and convection parameterisations – uncertainties in global modelling, *Atmos. Chem. Phys.*, 7, 4553–4568, 2007b, <http://www.atmos-chem-phys.net/7/4553/2007/>.
- Ulanovsky, A. E., Yushkov, V. A., Sitnikov, N. M., and Ravagnani, F.: The FOZAN-II fast-response chemiluminescent airborne ozone analyzer, *Instruments and Experimental Techniques*, 44, 249–256, 2001.
- v. Kuhlmann, R. and Lawrence, M. G.: The impact of ice uptake

- of nitric acid on atmospheric chemistry, *Atmos. Chem. Phys.*, 6, 225–235, 2006,
<http://www.atmos-chem-phys.net/6/225/2006/>.
- Vaughan, G., Schiller, C., MacKenzie, A., Bower, K., Peter, T., Schlager, H., Harris, N. R. P., and May, P. T.: SCOUT-O3/ACTIVE High-altitude Aircraft Measurements around Deep Tropical Convection, *Bullet. Amer. Meteor. Soc.*, 89, 647–662, 2008.
- Viciani, S., D’Amato, F., Mazzinghi, P., Castagnoli, F., Toci, G., and Werle, P.: A crygenically operated laser diode spectrometer for airborne measurement of stratospheric trace gases, *Applied Physics B*, 90, 581–592, 2008.
- Vignati, E., Wilson, J., and Stier, P.: M7: An efficient size-resolved aerosol microphysics module for large-scale aerosol transport models, *J. Geophys. Res.*, 109, D22202, doi:10.1029/2003JD004485, 2004.
- Wilcox, E. M.: Spatial and Temporal Scales of Precipitation Tropical Cloud Systems in Satellite Imagery and the NCAR CCM3, *J. Clim.*, 16, 3545–3559, 2003.
- Zhang, G. J. and McFarlane, N. A.: Sensitivity of Climate Simulations to the Parameterization of Cumulus Convection in the Canadian Climate Centre General Circulation Model, *Atmos.-Ocean*, 33, 407–446, 1995.
- Zhang, K., Wan, H., Zhang, M., and Wang, B.: Evaluation of the atmospheric transport in a GCM using radon measurements: sensitivity to cumulus convection parameterization, *Atmos. Chem. Phys.*, 8, 2811–2832, 2008,
<http://www.atmos-chem-phys.net/8/2811/2008/>.